OPEN ACCESS
Freely Available Online

JOURNAL OF ADVANCES IN NANOTECHNOLOGY
ISSN NO: 2689-2855

Research Article

DOI: 10.14302/issn.2689-2855.jan-19-2598

Influence Of Chemical Reaction on Marangoni Convective Flow of Nanoliquid in the Presence of Lorentz Forces and Thermal Radiation: A Numerical Investigation

Ghulam Rasool[1,*], Ting Zhang[1], Anum Shafiq[2], Hulya Durur[3]

[1]School of Mathematical Sciences, Zhejiang University, Hangzhou 310027, PR-China
[2]Department of Mathematics, Preston University, Islamabad 44000, Pakistan
[3]Department of Computer Engineering, Faculty of Engineering, Ardahan University, Ardahan, Turkey

Abstract

This study aims to numerically investigate the Marangoni convective flow of nanoliquid initiated by surface tension and heading towards a radiative Riga surface. The surface tension appears in the problem due to the gradients of temperature and concentration at the interface. The influence of first order chemical reaction is involved in the system with sufficient boundary conditions. Set of governing nonlinear PDEs is transformed into highly nonlinear ODEs using suitable transformations. HAM is applied for convergent series solutions. Impact of various pertinent fluid parameters on momentum, thermal and solutal boundary layers is analyzed graphically. The chemical reaction plays vital role in saturation of nanoparticles in the base fluid near the surface as well as away from it. The Lorentz forces originated by the Riga surface become powerful when the radiation parameter comes into effect. The significance of Riga plate is thus more prominent through thermal radiation. However, the magnetic effect dampens down for higher radiation parameter. Fluid parameters, Nusslt and Sherwood numbers are analyzed with detailed discussion and concluding remarks.

Corresponding author: Ghulam Rasool, School of Mathematical Sciences, Zhejiang University, Hangzhou 310027, PR-China, Email: grasool@zju.edu.cn

Keywords: Nanoparticles; Nanoliquid; Riga surface; Thermal radiation; Chemical reaction.

Received: Jan 10, 2019 **Accepted:** Feb 01, 2019 **Published:** Feb 08, 2019

Editor: Inder Kaur, Nottingham Trent university, UK.

Introduction

Carlo Marangoni, an Italian scientist introduced the concept of surface tension gradients driven fluid. This surface tension is popped up in the surface due to gradients of temperature and concentration on the occurrence of a liquid to liquid or liquid to air interface. A liquid with higher surface tension attracts more liquid from a region with low surface tension that ultimately results in fluid flow away from the regions having low surface tension. The gradients of temperature and concentration are therefore, critical factors for such convections under Marangoni effect. A significant interest developed in investigation of heat and mass convection under this phenomenon for its vast applications in industries such as welding, crystals, melting of electronic beams etc. Consequently, numerous researchers contributed in this field after Marangoni. Lin et al [1] worked on the convection under Marangoni phenomena with thermal gradients and magnetic number variation. Exact solutions achieved by Aly and Ebaid [2] in their study on Marangoni convection of nanoliquids achieved significant appreciation in nanoliquid convection analysis. Mat et al. [3], Gevorgyan et al. [4] and Al-sharafi et al. [5] have also contributed in this field of study with valuable results there in.

Engineers, Scientists working in the field of Nuclear energy, and Pharmaceutics come across the problem of rise in temperature in the working machine at a high speed performance. This situation was a big reason to worry in fluid mechanics before the introduction of Nanoliquids. The Idea of nanoliquid was introduced by Choi [6] in his research study. Pouring nanoparticles in a base fluid of poor conductivity showed drastically efficient results in the aspect of thermal conductivity of the base fluid. These impurities improved the conductivity of the fluid up to a significant level and the problem of machine heating was controlled with improved efficiency. Later on, Ibanez et al. [7] studied MHD nanoliquids analytically assuming convective boundary conditions. Hayat et al. [8] studied flow on stagnation point with an inclined magnetic field considering a nanofluid. Anum et al. [9] analyzed a third grade nanoliquid flow over a Riga plate with Cattaneo-Christov model in application. Hayat et al. [10] studied MHD-Powell-Eyring nanofluid flow with convective conditions. Alsabery et al. [11] studied heat flux in simulating the nanoliquid obtaining good results in Nusslt number. Numerous applications have been presented by Sheikholeslami and Ganji [12] in their research for useful nanoliquids. Nasrin et al. [13] studied free convection in aspect of nanoliquid passing through a chamber. Williamson nanoliquid has been analyzed by Bhatti and Rashidi [14]. Parvin et al. [15] studied free convection through curved cavity using water based nanoliquid. Selimefendigil and Oztop [16] studied conjugate convection via titled cavity. Reddy et al. [17] performed numerical simulations of the mixed convection using two phase fluid model through a plate. For more related works one can see [18-30].

Fluid flow analysis in the field of fluid mechanics has always been dependent on various external influencing agents. Researchers working in the field of Astrology and Geo physics always need such kind of external agents to ease the movement of fluid in their processing. Most of the fluids for example plasma are typically dependent on the magnetic induction for their flow phenomena. Reason of this dependence of fluids on external agents is poor conductivity of fluids. The problem was somehow reduced with the introduction of Riga plate, an array of permanently mounted magnets and alternating electrodes as displayed in the model of this paper. Gailitis and Lielausis [31] introduced this array in their study for the first time which is treated as a hallmark in the field of fluid mechanics. Later on, Ahmed et al. [32] studied the impacts of zero mass flux on fluids involving Riga plate in their model. Sheikholeslami et al. [33] in their research concluded that temperature profile shows decreasing behavior with strong Marangoni number (r) due to Lorentz forces. Shafiq et al. [34] studied fluid point-flow based Walters-B model involving a Riga plate in their study and found fruitful results in the aspect of thermal characteristics. Adeel et al. [35] analyzed mixed convection nanoliquids mounting a vertical Riga plate in the way of fluid flow with strong suction.

Numerous articles on nanoliquids are available in the literature in the context of heat and mass flux with different variables and different systematic approaches. However, the use of Riga plate for generation of magnetic effect together with effect of chemical reaction is not found in the literature as for as to the knowledge of the author that assures the novelty

of this research work. In this study, firstly we have involved the Riga plate to generate Lorentz forces in the system. The chemical reaction effect and thermal radiation effect are considered. Secondly, the set of PDEs is converted into set of nonlinear ODEs with transformations using the technique of non-dimensionalization [36]. The non-dimensionalized system is subjected to HAM [37-42] for convergent series solutions. Thirdly, the convergence of the results is analyzed graphically and finally, the results are plotted with sufficient discussion on the behavior of flow profiles.

Mathematical Model

A two dimensional steady and in-compressible nanoliquid is considered under Marangoni effect heading towards a radiative Riga surface. The flow is driven by tension appearing in the surface due to the temperature and concentration gradients. Thermal radiation and chemical reaction effects are utilized. The Brownian motion factor and Thermphoresis phenomena are of significant importance in this study. The temperature T_f relates the temperature gradient whereas C_f relates the concentration gradient with base fluid. The heat-mass flux is considered along x-axis in Cartesian coordinates. Fig. 1 displays the physical scenario for the aforementioned problem. The governing equations are therefore:

$$\frac{\partial u}{\partial x}+\frac{\partial v}{\partial y}=0, \tag{1}$$

$$u\frac{\partial u}{\partial x}=v\frac{\partial^2 u}{\partial y^2}-v\frac{\partial u}{\partial y}+\frac{\pi j_0 M_0 \exp\left(\frac{-\pi y}{a}\right)}{8\rho_f}, \tag{2}$$

$$u\frac{\partial T}{\partial x}=\alpha\frac{\partial^2 T}{\partial y^2}-v\frac{\partial T}{\partial y}+\tau\left(D_B\frac{\partial C}{\partial y}\frac{\partial T}{\partial y}+\frac{D_T}{T_\infty}\left(\frac{\partial T}{\partial y}\right)^2\right)-\frac{1}{(\rho c)_f}\frac{\partial q_r}{\partial y}, \tag{3}$$

$$u\frac{\partial C}{\partial x}=D_B\frac{\partial^2 C}{\partial y^2}-v\frac{\partial C}{\partial y}+\frac{D_T}{T_\infty}\left(\frac{\partial T}{\partial y}\right)^2-K(C-C_\infty). \tag{4}$$

The surface tension s, being a function of T and C can be defined as follows:

$$\sigma=\sigma_0[1-\gamma_c(C-C_\infty)-\gamma_T(T-T_\infty)], \tag{5}$$

where

$$\gamma_C=-\frac{1}{\sigma_0}\frac{\partial\sigma}{\partial C}_T,\quad \gamma_T=-\frac{1}{\sigma_0}\frac{\partial\sigma}{\partial T}_C, \tag{6}$$

with following boundary conditions,

$$u(x,\infty)\to 0,\ T(x,\infty)\to T_\infty,\ C(x,\infty)\to C_\infty,\ v(x,0)=0,\ T(x,0)=T_\infty+T_0X^2,\ C(x,0)=C_\infty+C_0X^2,$$

$$\mu\frac{\partial u}{\partial y}_{y=0}=-\frac{\partial\sigma}{\partial x}_{y=0}=\sigma_0\left(\gamma_C\frac{\partial C}{\partial x}_{y=0}+\gamma_T\frac{\partial T}{\partial x}_{y=0}\right), \tag{7}$$

Here u, v represent the velocity components in x, y directions, respectively. μ is symbol of dynamic viscosity, ν is the kinematic viscosity, ρ_f represents the density of fluid, K is used for chemical reaction, σ the surface tension, T_0 and C_0 are temperature and concentration on the surface, α is representing thermal diffusivity of the fluid, k is symbol of thermal conductivity of fluid. τ is used for ratio between heat capacity of the ,

fluid, k is symbol of thermal conductivity of fluid. τ is used for ratio between heat capacity of the nanoparticles $(PC)_p$ and heat capacity of base fluid, $(PC)_f$, D_B is Brownian diffusion, D_T is Thermophoresis, and q_r is the typical radiative heat flux that can be written through Rosseland's approximation as follows:

$$q_r = \frac{-4\Sigma^*}{3k^*}\frac{\partial(T^4)}{\partial y}, \qquad (8)$$

where Σ^* and K^* are Stefan-Boltzmann's constant and coefficient of mean absorption, respectively. Using Taylor's series and omitting second and higher order terms, we get,

$$T^4 \cong 4T_\infty^3 T - 3T_\infty^4, \qquad (9)$$

which upon substitution in (8) yields

$$\frac{\partial q_r}{\partial y} = \frac{-16\Sigma^* T_\infty^3}{3k^*}\frac{\partial^2 T}{\partial y^2}, \qquad (10)$$

Equation (10) in (3) gives,

$$u\frac{\partial T}{\partial x} = \alpha\frac{\partial^2 T}{\partial y^2} - v\frac{\partial T}{\partial y} + \tau\left(D_B\frac{\partial C}{\partial y}\frac{\partial T}{\partial y} + \frac{D_T}{T_\infty}\left(\frac{\partial T}{\partial y}\right)^2\right) + \frac{-16\Sigma^* T_\infty^3}{3k^*}\frac{\partial^2 T}{\partial y^2}, \qquad (11)$$

Define,

$$C = C_0 X^2\phi(\eta) + C_\infty,\ T = T_0 X^2\theta(\eta) + T_\infty,\ \psi = \frac{\mu}{\rho}Xf(\eta),$$
$$\eta = \frac{y}{L},\ u(x,y) = \frac{\partial\psi}{\partial y},\ v(x,y) = -\frac{\partial\psi}{\partial x}, \qquad (12)$$

We obtain,

$$f''' - f'^2 + ff'' + Q\exp(-\beta\eta) = 0, \qquad (13)$$

$$\left(1 + \frac{4}{3}Rd\right)\theta'' + \Pr\left(f\theta' - 2f'\theta + N_t\theta'^2 + N_b\theta'\phi'\right) = 0, \qquad (14)$$

$$\phi'' + \mathrm{Sc}(f\phi' - 2f'\phi - K\phi) + \frac{N_t}{N_b}\theta'' = 0, \qquad (15)$$

with,

$$f(0) = 0,\ f''(0) = -2(1+r),\ \theta(0) = 1,\ \phi(0) = 1,$$
$$f'(\infty) = 0,\ \theta(\infty) = 0 = \phi(\infty), \qquad (16)$$

where $\boldsymbol{\gamma}$ = $(C_0\boldsymbol{\gamma}_C)$ / $(T_0\boldsymbol{\gamma}_T)$ is the ratio of thermal to solutal surface tension s.t. $R=((C_0-C_\infty)\gamma C)/((T_0-T_\infty)\gamma T)$ and $Ma|_{L,T} = (L\boldsymbol{\Delta}T\boldsymbol{\gamma}_T|_C)/\ \nu\alpha$, $Ma|_{L,C} = (L\boldsymbol{\Delta}C\gamma_{C|T})/\nu\alpha$ are thermal and solutal Marangoni numbers resulting $\boldsymbol{\gamma} = Ma|L,T\ /\ Ma|L,C$ is the Marangoni ratio. $(Q = L^4\ \pi j_0\ M_0/8\nu^2\ x\rho)$ is the modified Hartman number, $(\Pr = \nu/\alpha)$ is the Prandtl number, $(N_b = (\rho c)_p\ D_B\ C_0\ x^2\ /\ (\rho c)_f\ L^2\ a)$ is the Brownian motion factor, $\mathrm{Sc} = \nu/D$ is the Schmidt number, $(N_t = (\rho c)_p\ D_T\ x^2)\ /\ (\rho c)_f\ L^2\ a\ )$ is Thermophoretic factor, $(Rd = 4\Sigma^*\ T_\infty^3/\ kk^*)$, is radiation parameter and, $(\beta = \pi L/a)$ is dimensionless parameter. Skin friction coefficient, local Nusselt and Sherwood numbers are defined by,

$$Re_x^{1/2} C_{fx} = (2f'(0)), \quad Re_x^{-1/2} Nu_x = -\left(1 + \tfrac{4}{3} Rd\right)\theta'(0), \quad Re_x^{-\frac{1}{2}} Sh_x = -\phi'(0), \qquad (17)$$

where $Re_x = ux/v$ represents the local Reynolds number.

Numerical Simulation

The efficiency of Homotopy analysis method (HAM) for solving non-linear ODEs has been witnessed through literature. Researchers have given preference to this technique over various other famous methods. The method starts with assumption of some suitable initial guess subject to the boundary conditions given in the problem. Let,

$$f_0 = 2(1 - e^{-\eta})(1 + r), \quad \theta_0 = e^{-\eta}, \quad \phi_0 = e^{-\eta}. \qquad (18)$$

One can see that (16) is satisfied. Define,

$$\ell_f = \frac{\partial^3 f}{\partial \eta^3} - \frac{\partial f}{\partial \eta}, \quad \ell_\theta = \frac{\partial^2 \theta}{\partial \eta^2} - \theta, \quad \ell_\phi = \frac{\partial^2 \phi}{\partial \eta^2} - \phi, \qquad (19)$$

such that,

$$\hat{\ell}_f[a_1 e^{-\eta} + a_2 e^{\eta} + a_3] = 0, \quad \hat{\ell}_\theta[a_4 e^{-\eta} + a_5 e^{\eta}] = 0, \quad \hat{\ell}_\phi[a_6 e^{-\eta} + a_7 e^{\eta}] = 0, \qquad (20)$$

Where a_i are constants for. i = 1-7. The 0^{th} order deformation problems are:

$$\frac{1-p}{p\hat{h}_f} \ell_f[\hat{f}(\eta, p) - f_0(\eta)] = N_f[\hat{f}],$$

$$\frac{1-p}{p\hat{h}_\theta} \ell_\theta[\hat{\theta}(\eta, p) - \theta_0(\eta)] = N_\theta[\hat{f}, \hat{\theta}, \hat{\phi}],$$

$$\frac{1-p}{p\hat{h}_\phi} \ell_\phi[\hat{\phi}(\eta, p) - \phi_0(\eta)] = N_\phi[\hat{f}, \hat{\theta}, \hat{\phi}], \qquad (21)$$

subject to,

$$\hat{\theta}(0,p) = 1, \ \hat{\phi}(0,p) = 1, \ \hat{f}(0,p) = 0, \ \frac{\partial \hat{f}(0,p)}{\partial \eta^2} = -2(1+r),$$
$$\frac{\partial \hat{f}(\infty,p)}{\partial \eta} = 0, \ \hat{\theta}(\infty,p) = 0, \ \hat{\phi}(\infty,p) = 0. \qquad (22)$$

Resulting the following system,

$$N_f[\hat{f}] = \frac{\partial^3 \hat{f}}{\partial \eta^3} + \hat{f}\frac{\partial^2 \hat{f}}{\partial \eta^2} - \left(\frac{\partial \hat{f}}{\partial \eta}\right)^2 + Q\exp(-\beta\eta),$$
$$N_\theta[\hat{f}, \hat{\theta}, \hat{\phi}] = \left(1 + \tfrac{4}{3} Rd\right)\frac{\partial^2 \hat{\theta}}{\partial \eta^2} + \Pr\left(\hat{f}\frac{\partial \hat{\theta}}{\partial \eta} - 2\hat{\theta}\frac{\partial \hat{f}}{\partial \eta} + N_b \frac{\partial \hat{\theta}}{\partial \eta}\frac{\partial \hat{\phi}}{\partial \eta} + N_t\left(\frac{\partial \hat{\theta}}{\partial \eta}\right)^2\right),$$
$$N_\phi[\hat{f}, \hat{\theta}, \hat{\phi}] = \frac{\partial^2 \hat{\phi}}{\partial \eta^2} + Sc\left(\hat{f}\frac{\partial \hat{\phi}}{\partial \eta} - 2\frac{\partial \hat{f}}{\partial \eta}\hat{\phi} - K\hat{\phi}\right) + \frac{N_t}{N_b}\frac{\partial^2 \hat{\theta}}{\partial \eta^2}, \qquad (23)$$

where $p \in [0,1]$ is a typical embedding parameter and $\hat{\mathbf{h}}_f, \hat{\mathbf{h}}_\theta, \hat{\mathbf{h}}_\phi$ are so-called auxiliary parameters with N_f, N_θ, N_ϕ are the non-linear operators. For $p=0,1$, we have:

$$\hat{f}(\eta,0) = f_0, \ \hat{f}(\eta,1) = f, \ \hat{\theta}(\eta,0) = \theta_0, \ \hat{\theta}(\eta,1) = \theta, \ \hat{\phi}(\eta,0) = \phi_0, \ \hat{\phi}(\eta,1) = \phi. \qquad (24)$$

Using Taylor's expansion,

$$\hat{f} = \sum_{m=0}^{\infty} f_m(\eta)p^m,\ \hat{\theta} = \sum_{m=0}^{\infty} \theta_m(\eta)p^m,\ \hat{\phi} = \sum_{m=0}^{\infty} \phi_m(\eta)p^m. \quad (25)$$

The convergence of (24) is purely dependent on the choice of $\hbar$. For p such that the system (24) converges, we write,

$$\sum_{m=0}^{\infty} f_m(\eta) = f = f_0 + \sum_{m=1}^{\infty} f_m,$$
$$\sum_{m=0}^{\infty} \theta_m(\eta) = \theta = \theta_0 + \sum_{m=1}^{\infty} \theta_m,$$
$$\sum_{m=0}^{\infty} \phi_m(\eta) = \phi = \phi_0 + \sum_{m=1}^{\infty} \phi_m \quad (26)$$

The m^{th} order deformation problems are,

$$l_f[f_m - \Phi_m f_{m-1}] = \hbar_f R_f^m,\ l_\theta[\theta_m - \Phi_m \theta_{m-1}] = \hbar_\theta R_\theta^m,\ l_\phi[\phi_m - \Phi_m \phi_{m-1}] = \hbar_\phi R_\phi^m, \quad (27)$$

where $\phi_m=1$ for $m>1$ otherwise 0. Finally,

$$R_f^m = \frac{\partial^3 f_{m-1}}{\partial \eta^3} + \sum_{k=1}^{m-1} f_{m-1-k}\frac{\partial^2 f_k}{\partial \eta^2} - \sum_{k=0}^{m-1}\frac{\partial f_{m-1-k}}{\partial \eta}\frac{\partial f_k}{\partial \eta} + Q\exp(-\beta\eta),$$
$$R_\theta^m = \left(1+\frac{4}{3}Rd\right)\frac{\partial^2 \theta_{m-1}}{\partial \eta^2} + \Pr\left(\sum_{k=0}^{m-1} f_{m-1-k}\frac{\partial \theta_k}{\partial \eta} - 2\sum_{k=0}^{m-1}\theta_{m-1-k}\frac{\partial f_k}{\partial \eta} + N_b\sum_{k=0}^{m-1}\frac{\partial \theta_{m-1-k}}{\partial \eta}\frac{\partial \phi_k}{\partial \eta} + N_t\sum_{k=0}^{m-1}\frac{\partial \theta_{m-1-k}}{\partial \eta}\frac{\partial \theta_k}{\partial \eta}\right),$$
$$R_\phi^m = \frac{\partial^2 \phi_{m-1}}{\partial \eta^2} + Sc\left(\sum_{k=0}^{m-1} f_{m-1-k}\frac{\partial \phi_k}{\partial \eta} - 2\sum_{k=0}^{m-1}\frac{\partial f_{m-1-k}}{\partial \eta}\phi_k - K\phi_{m-1}\right) + \frac{N_t}{N_b}\sum_{k=0}^{m-1}\frac{\partial \theta_{m-1-k}}{\partial \eta}\frac{\partial \theta_k}{\partial \eta}, \quad (28)$$

with following general solutions to the problem,

$$f_m = a_1 + a_2 e^{\eta} + a_3 e^{-\eta} + f_m^*(\eta),$$
$$\theta_m = a_4 e^{\eta} + a_5 e^{-\eta} + \theta_m^*(\eta),$$
$$\phi_m = a_6 e^{\eta} + a_7 e^{-\eta} + \phi_m^*(\eta), \quad (29)$$

where a_i are constants for i =1-7 and $f_m^*(\eta)$, $\theta_m^*(\eta)$, $\phi_m^*(\eta)$ are special solutions.

Convergence of Solutions

The auxiliary parameters used for the flow profiles in series solutions in HAM are typically considered for controlling the convergence. These parameters significantly moderate the convergence rates thus are vital in achieving the convergence of final solutions. Convergence interval of f, θ and ϕ are sketched in Fig. 2. One can see that the intervals of convergence for the aforementioned three profiles are [-0.40, 0.05], [-0.45, 0.05] and [-0.45, 0.05], respectively. The solutions show convergence after 19^{th} iteration for velocity profile and 26^{th} iteration for temperature and concentration profiles, respectively.

Results and Discussion

We examine the behavior of a surface tension driven nanofluid under the action of Lorentz forces generated by Riga surface and the chemical reaction inside the fluid. The flow is assumed in two dimensions such that x-axis is parallel to the fluid flow and y-axis is normal to the surface of the Riga plate. Influence of pertinent fluid parameters on flow profiles is plotted graphically and the discussion on these graphs is as follows. Fig. 3 presents the behavior of velocity profile with variation in the dimensionless parameter β. The elevated values of β enhance the fluid viscosity that results in decreasing the flow momentum and corresponding boundary layer drops down. The flow

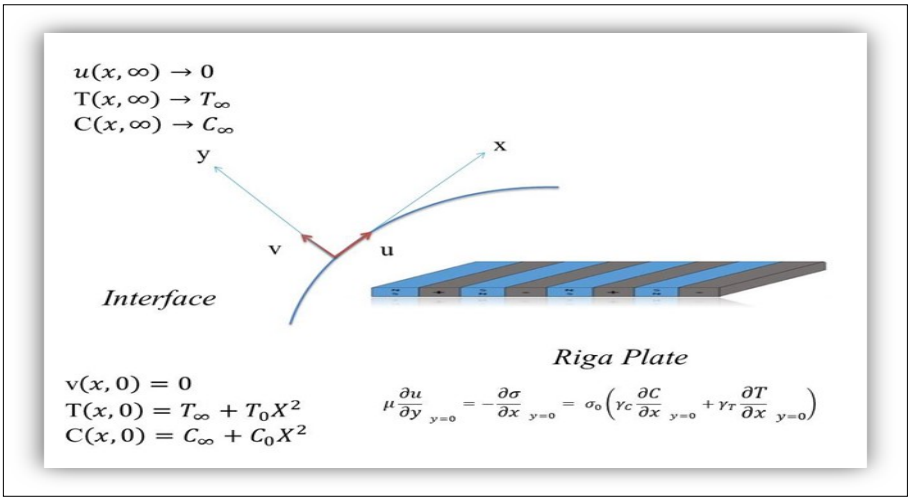

Figure 1. Schematic Diagram

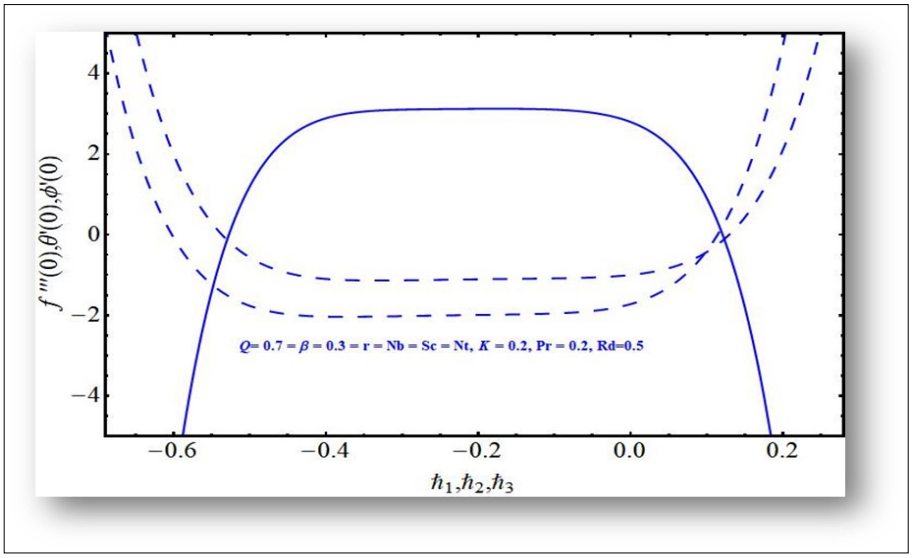

Figure 2. H-Curves for Velocity, Temperature and Concentration Profiles

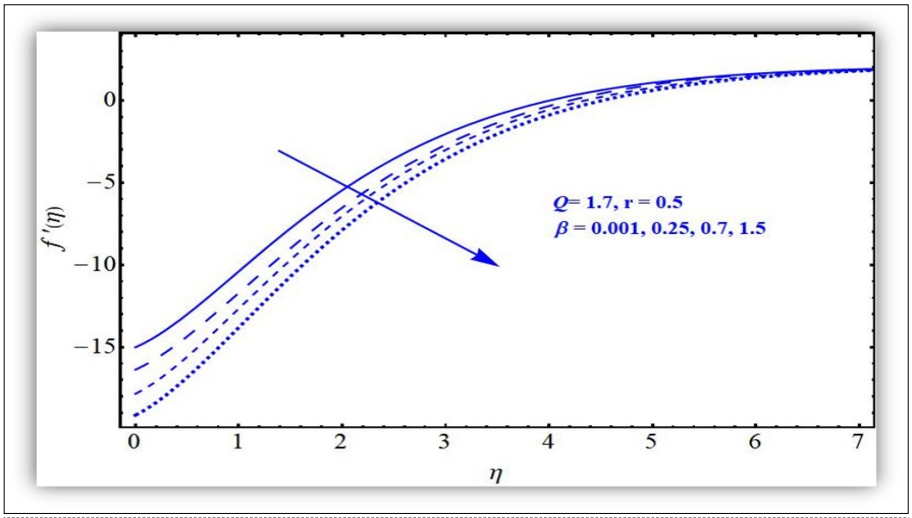

Figure 3. Velocity profile against ß

velocity receives enhancement with elevated values of modified Hartman number as displayed in Fig. 4. The graph of $f'(\eta)$ shows augmented variation with augmented values of. Q The induced Lorentz forces parallel to the flow profile enhance the surface tension produced in fluid that certainly drives the fluid with stronger force. Consequently the flow profile receives an increasing behavior. Fig. 5 shows the behavior of velocity profile and associated boundary layer with variation in Marangoni ratio (r). One can see an increasing behavior in profile for elevated values of r. Fig. 6 is the display of temperature profile against the dimensionless parameter β. The temperature drops down for elevated values of β. The rise in viscosity for elevated values of β results in slow motion of fluid and consequently lessens the collisions in between fluid particles as well as between fluid particles and nanoparticles that results in decreasing behavior of temperature profile. The same is noticed with augmented values of Q plotted in Fig. 7. The temperature profile and associated boundary layer shows a decreasing behavior. A significantly prominent increase in temperature profile is witnessed for larger values of Prandtl number (Pr) portrayed in Fig. 8. Since, Prandtl number is the ratio of momentum diffusivity to thermal diffiusivity, therefore, the elevated values of Pr number enhance the momentum diffusivisity that results in enhancement of temperature profile and associated boundary layer. Not prominent, but comparatively an increasing behavior is noticed in temperature profile with enhancement in Thermophoretic factor (Nt) as plotted in Fig. 9. The enhancement is dependent on the strong Thermophoretic force that results the away

movement of nanoparticles from the surface of Riga. Fig. 10 is the display of influence of radiation factor (Rd) on the temperature profile. Temperature profile receives prominent enhancement in its behavior with elevated values of radiation factor. Thus the addition of radiation factor enhances the heat flux up to a significant level. Fig. 11 is plotted to analyze the behavior of concentration of nanoparticles against the variation in Brownian motion factor (Nb). The stronger Brownian motion factor enhances the in-predictive motion of fluid particles that results in enhancement of temperature distribution. This enhancement in temperature drops down the concentration of nanoparticles near the Riga surface. The concentration profile enhances with elevated values of Schmidt number (Sc) for certain reasons as shown in Fig. 12. The main reason is the enhancement in Brownian diffusivity that results in enhancement of associated boundary layer of concentration of nanoparticles in the base fluid. Elevated values of both the chemical reaction and radiation factor result in decreasing behavior of the concentration profile displayed in Fig. 13 and Fig. 14, respectively. The enhancement in chemical reaction results in away movement of nanoparticles from the surface that ultimately effects the concentration in the base fluid. The elevated values of Thermophoretic factor (Nt) result in enhancement of heat flux but drops down the mass flux while the enhancement in Prandtl results in decreasing behavior of the Sherwood number (the mass flux) as plotted in Fig. 15, 16 and 17.

Comparison

This subsection summarizes the result with a precise comparison of present results with [33]. Setting M=0 in [33] and Q=0=K=Rd in present model, the left over system of equations and the graphical results are exactly the same in either case as presented in Fig. 18 for the velocity profile against Marangoni ratio (r). However, considering the effects of Q, K and Rd, we observe that there is a significant variation in the graphical results in the present work as compared to the previous work. For example, the elevated values of γ result in a rapid increasing behavior of velocity profile in the present case as compared to [33] confirming a more prominent effect of Marangoni ratio (r) on the flow profiles.

Closing Remarks

We examine the behavior of a surface tension driven nanofluid under the action of Lorentz forces generated by Riga surface and the chemical reaction inside the fluid. The flow is assumed in two dimensions such that x-axis is parallel to the fluid flow and y-axis is normal to the surface of the Riga plate. The final governing equations after application of suitable transformations with sufficient boundary conditions have been solved by HAM. The convergent series solutions are presented and analyzed graphically. Following are salient conclusions

- Velocity profiles receives prominent enhancement

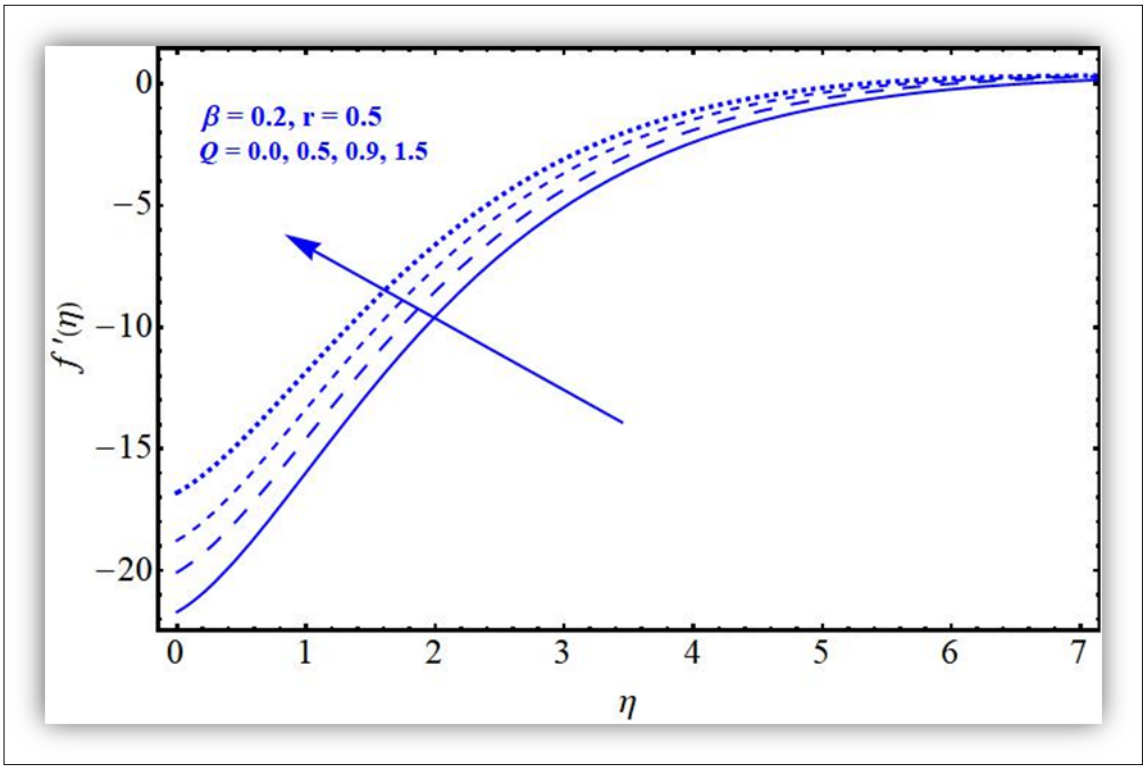

Figure 4. Velocity profile against Q

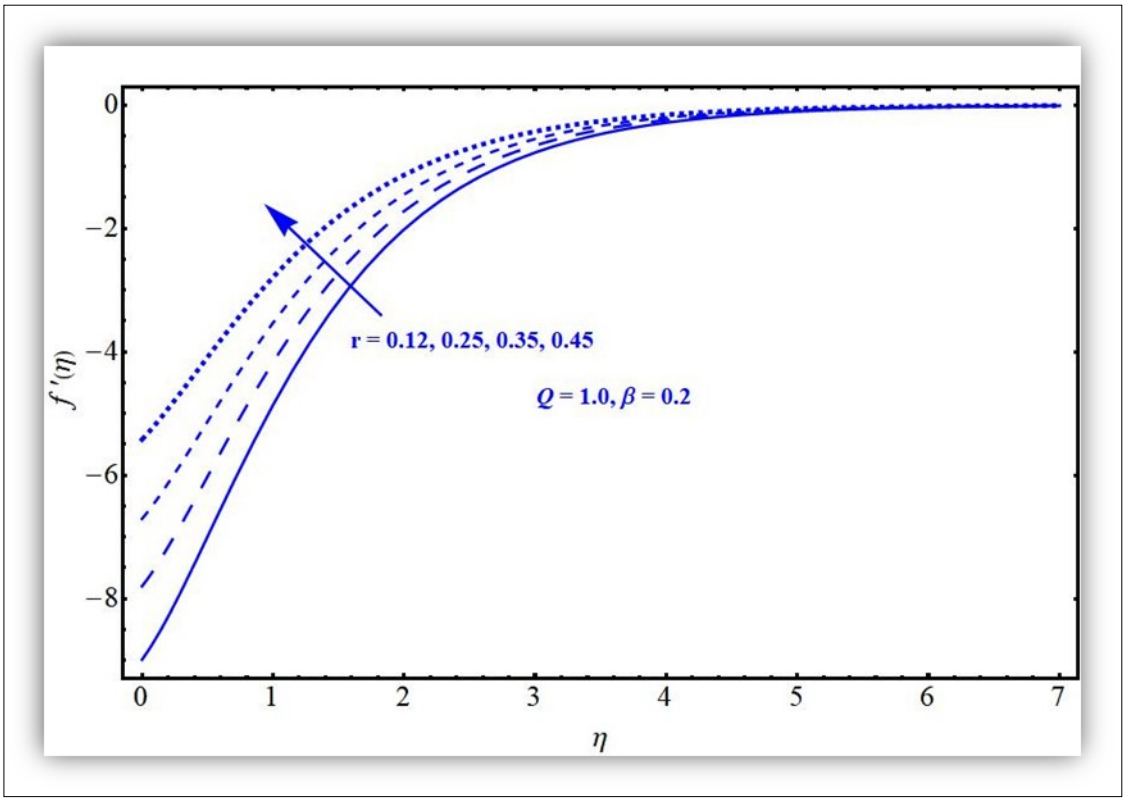

Figure 5. Velocity Profile against r

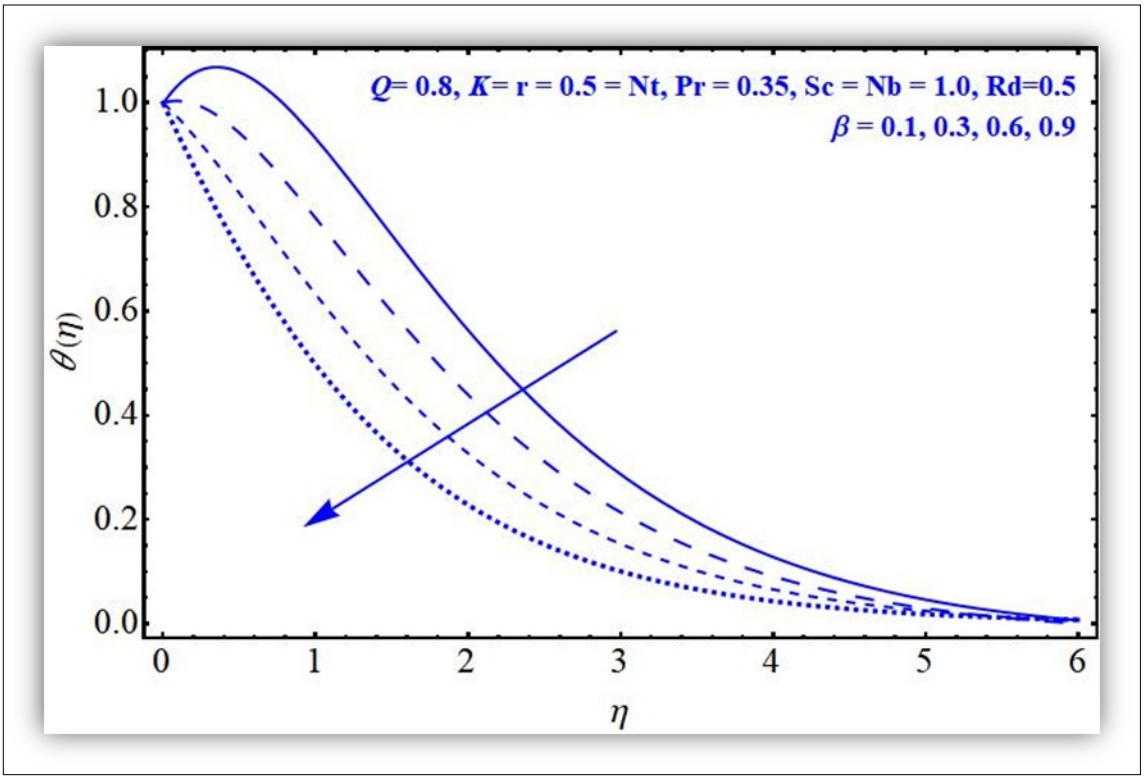

Figure 6. Temperature profile against ß

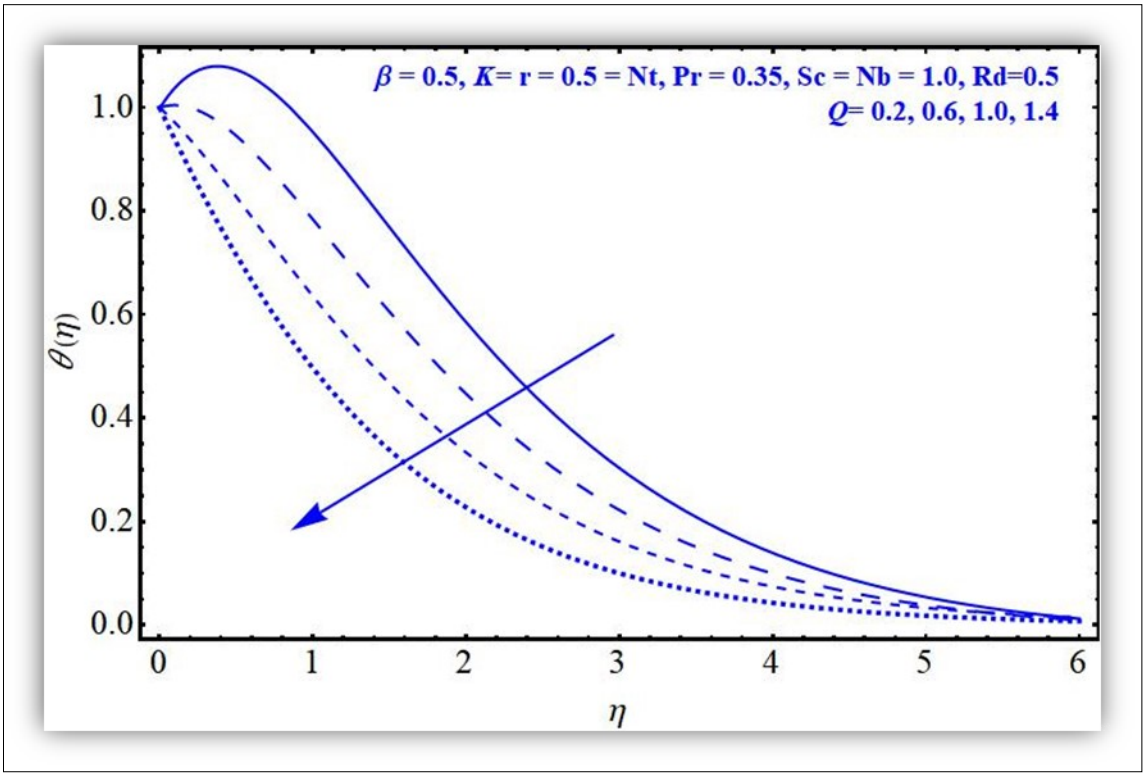

Figure 7. Temperature profile against Q

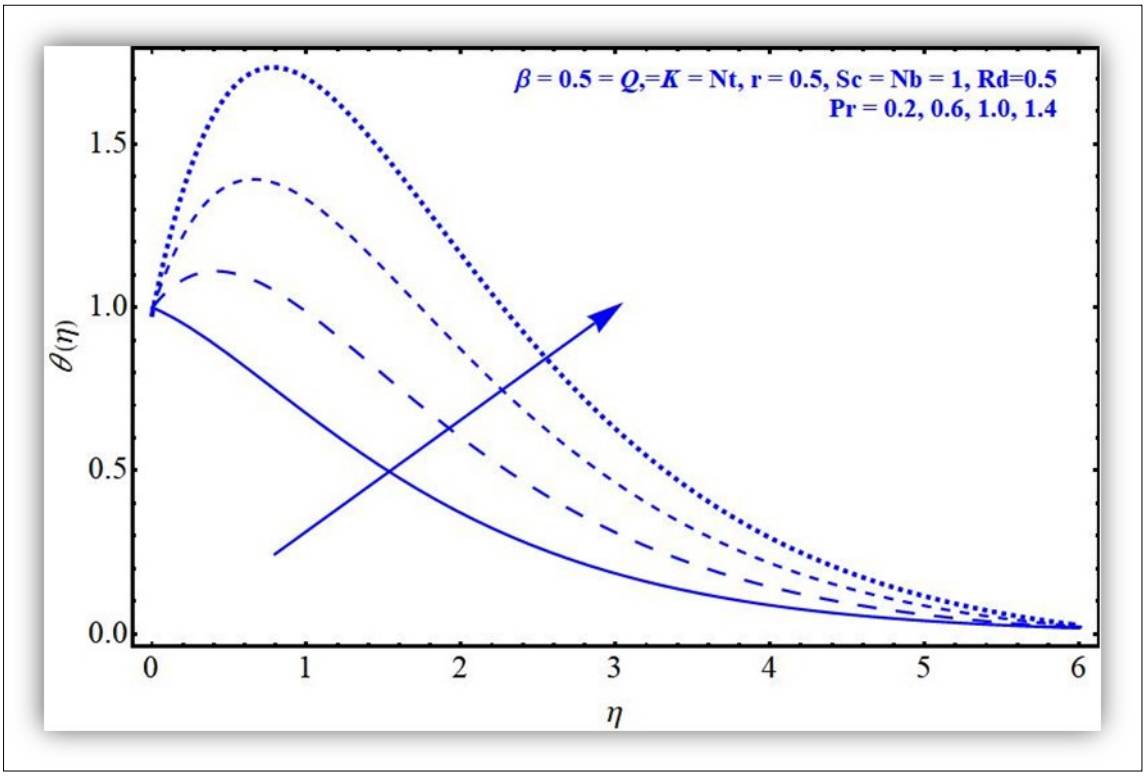

Figure 8. Temperature profile against Pr

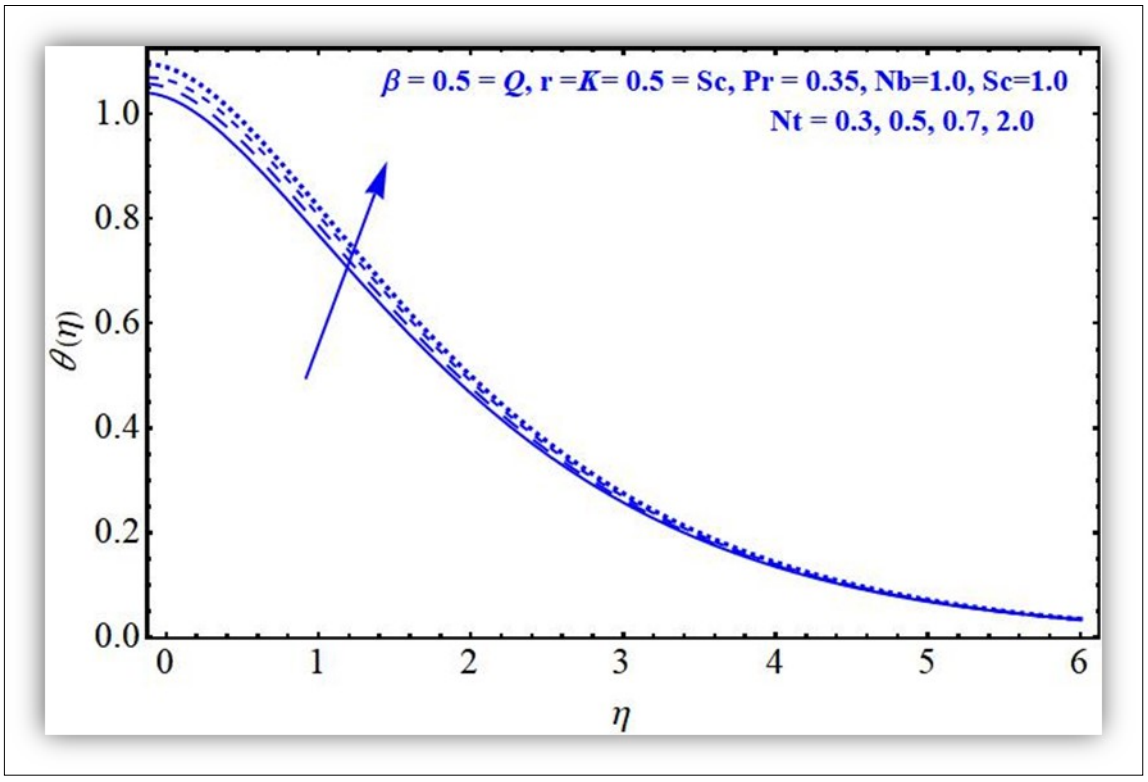

Figure 9. Temperature profile against Nt

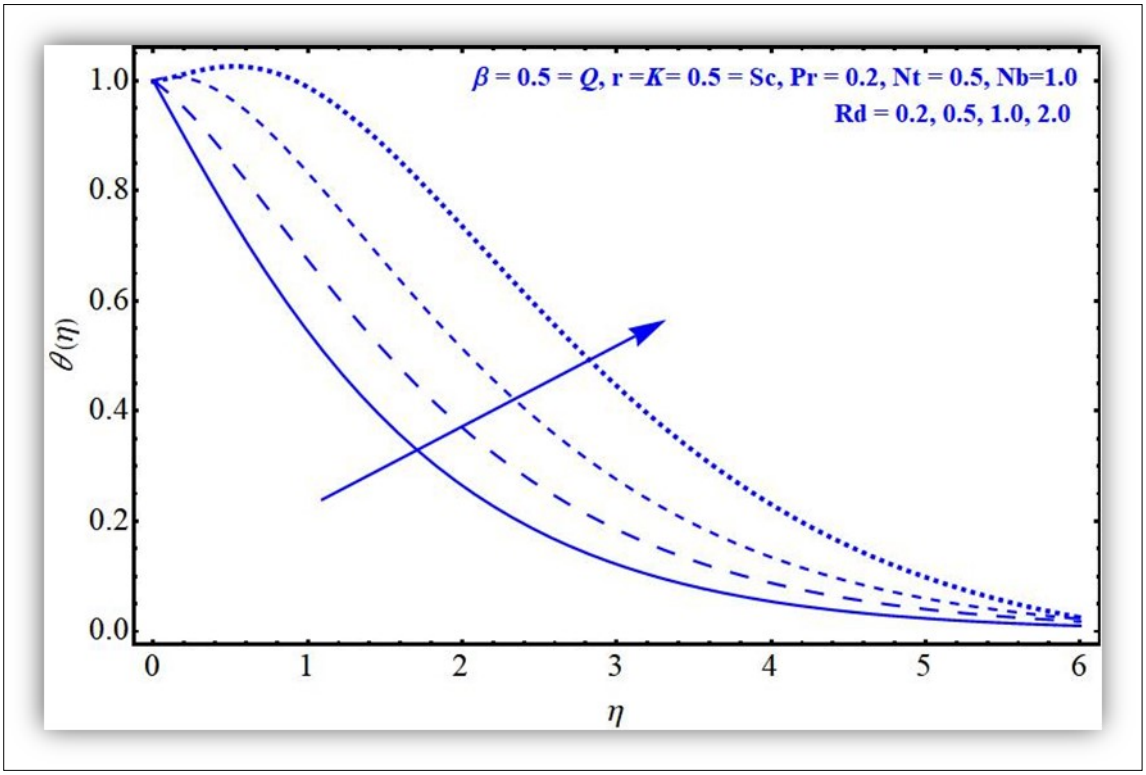

Figure 10. Temperature profile against Rd

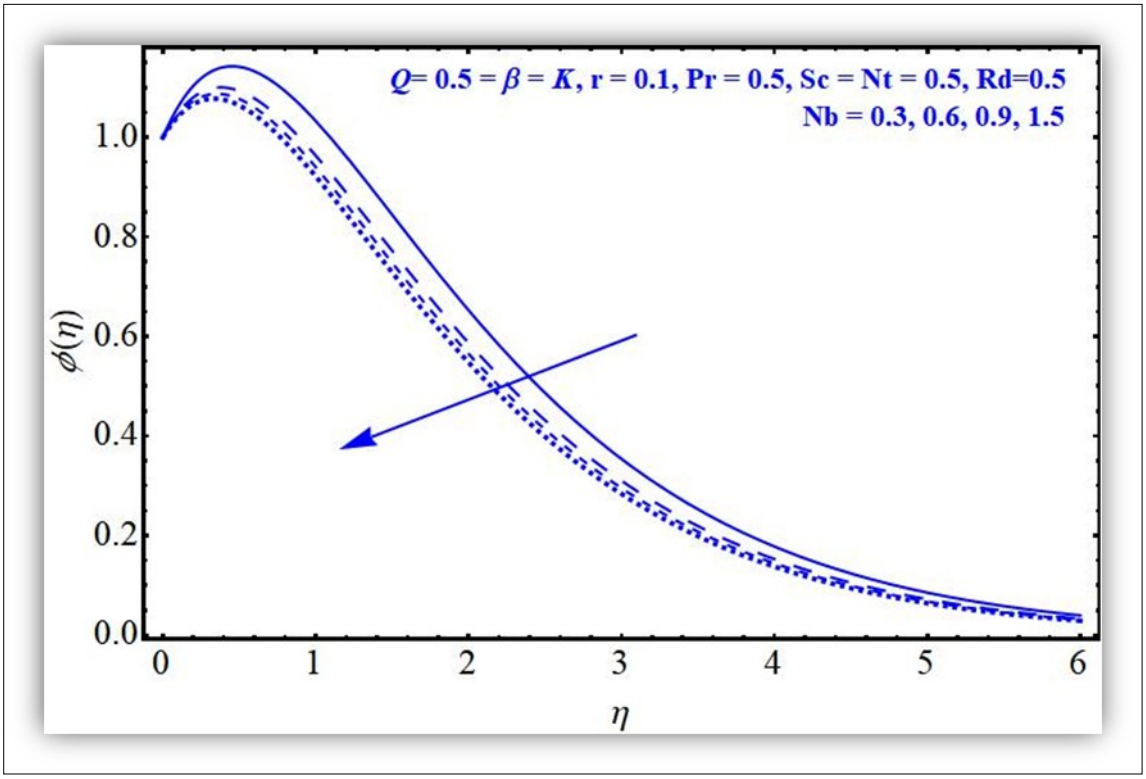

Figure 11. Concentration profile against Nb

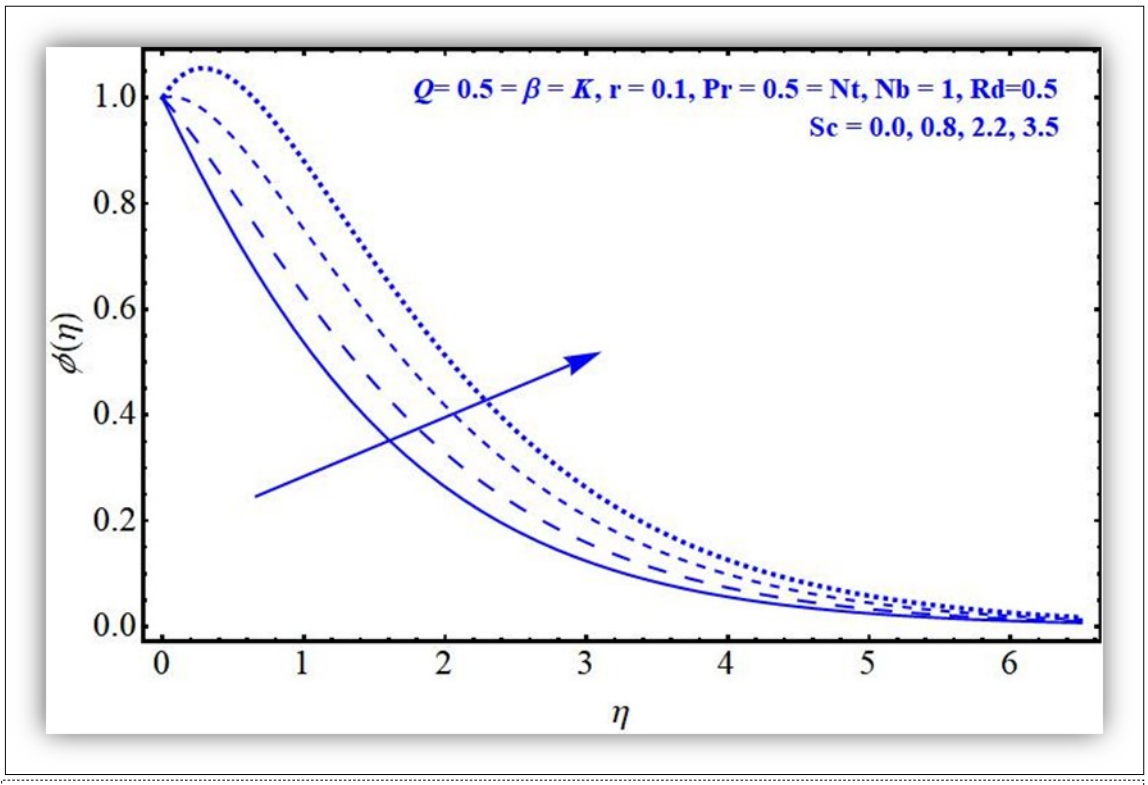

Figure 12. Concentration profile against Sc

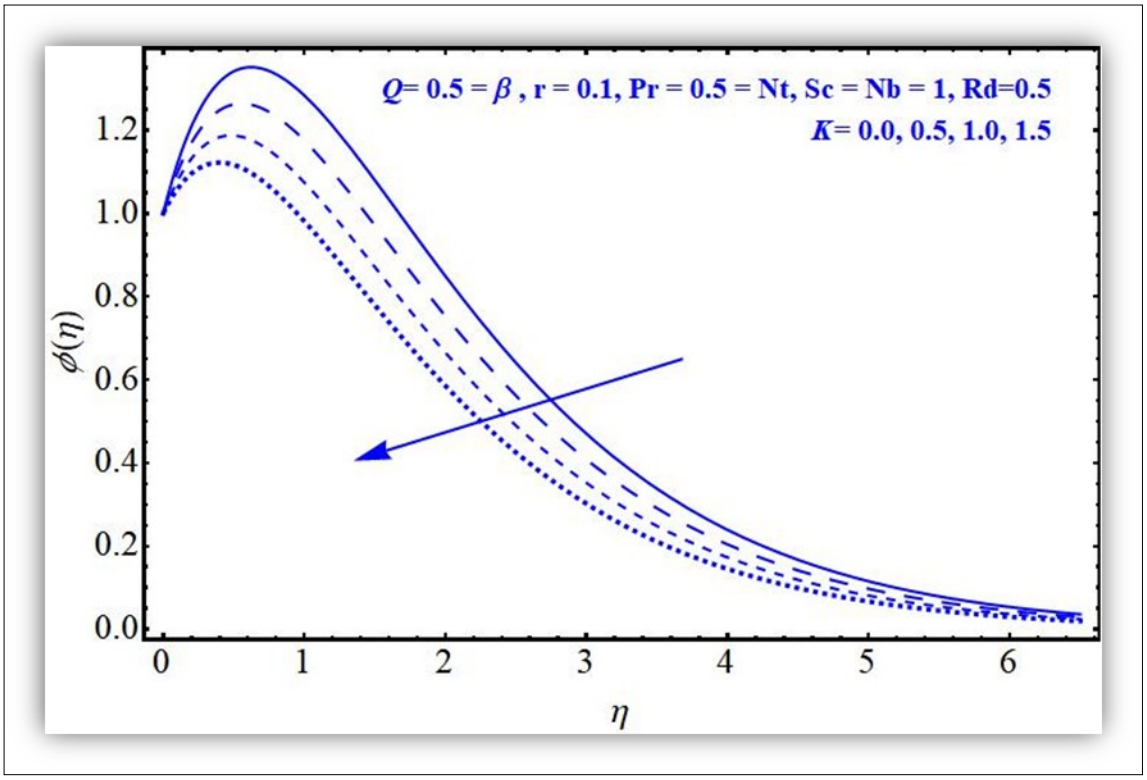

Figure 13. Concentration profile against K

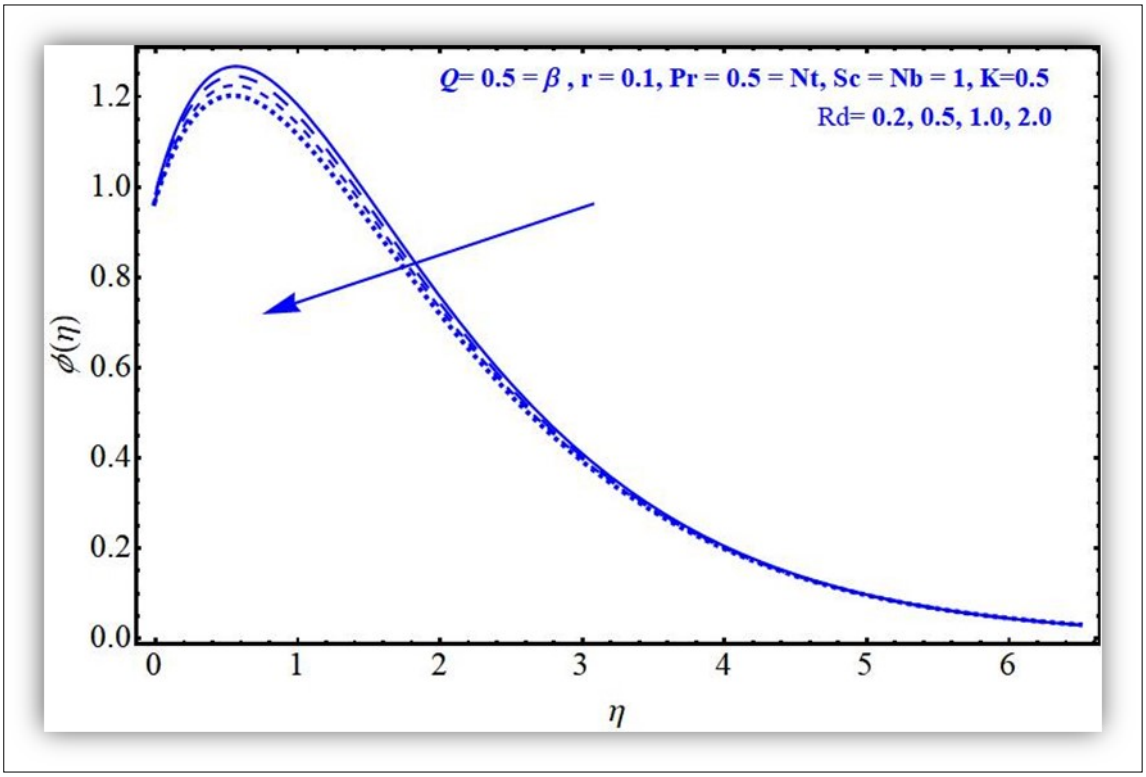

Figure 14. Concentration profile against Rd

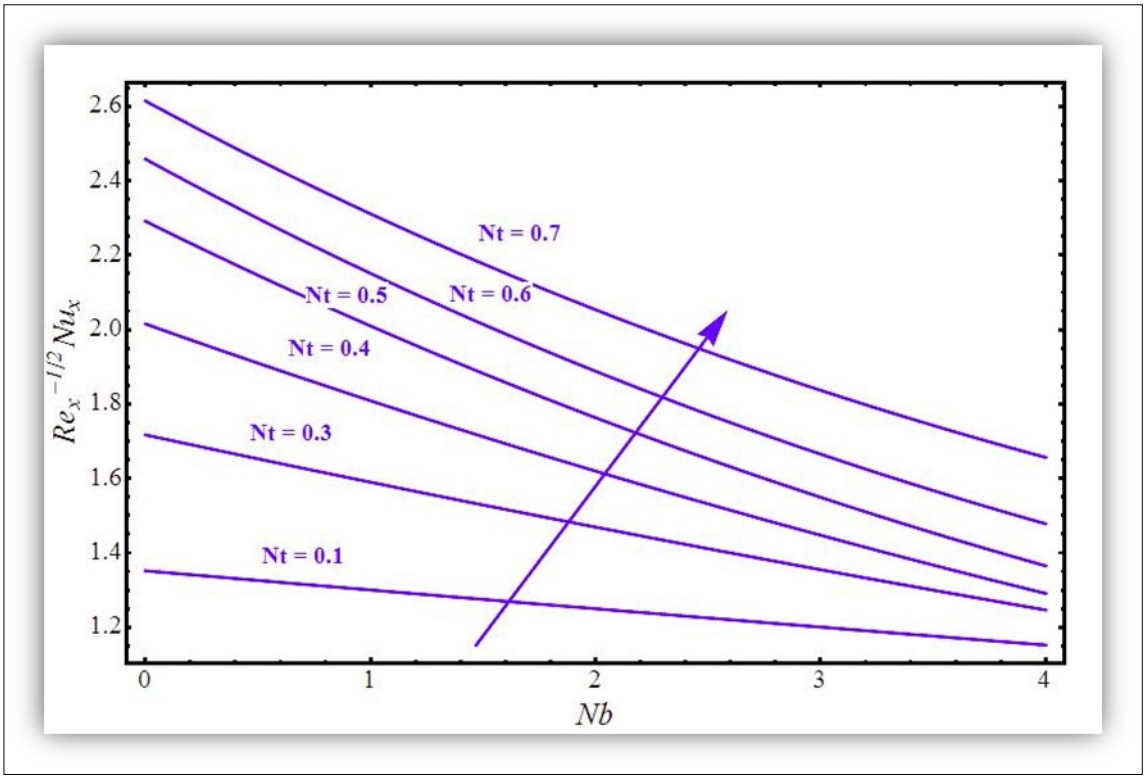

Figure 15. Nusslt number against Nb

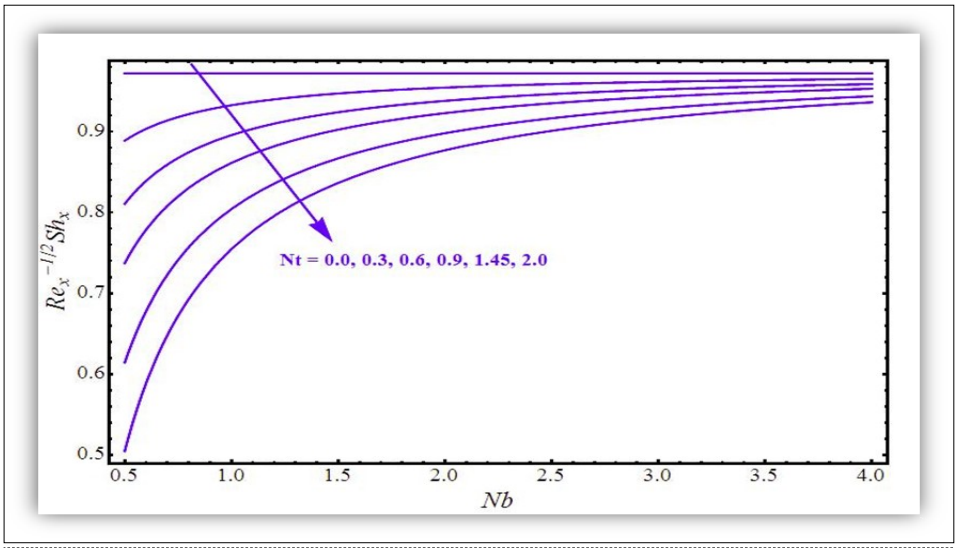

Figure 16. Sherwood number against Nb

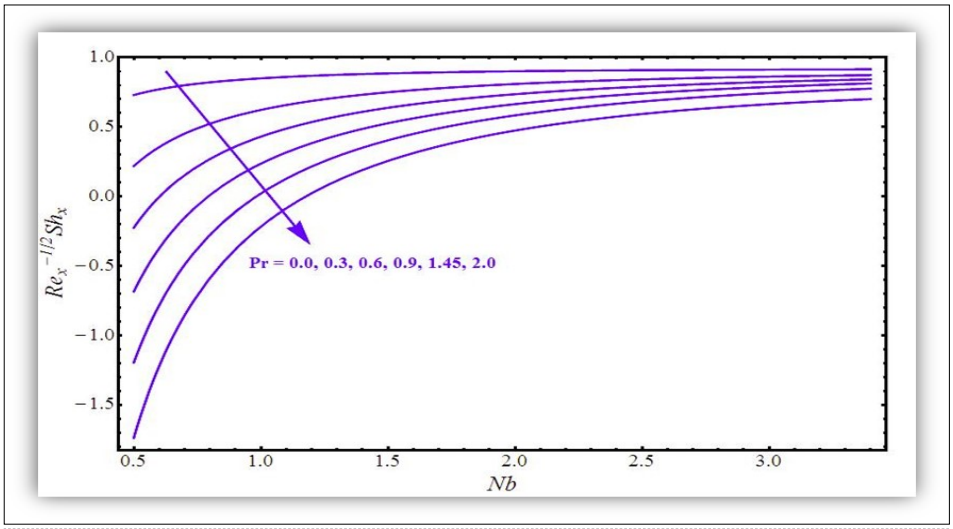

Figure 17. Sherwood number against Nb

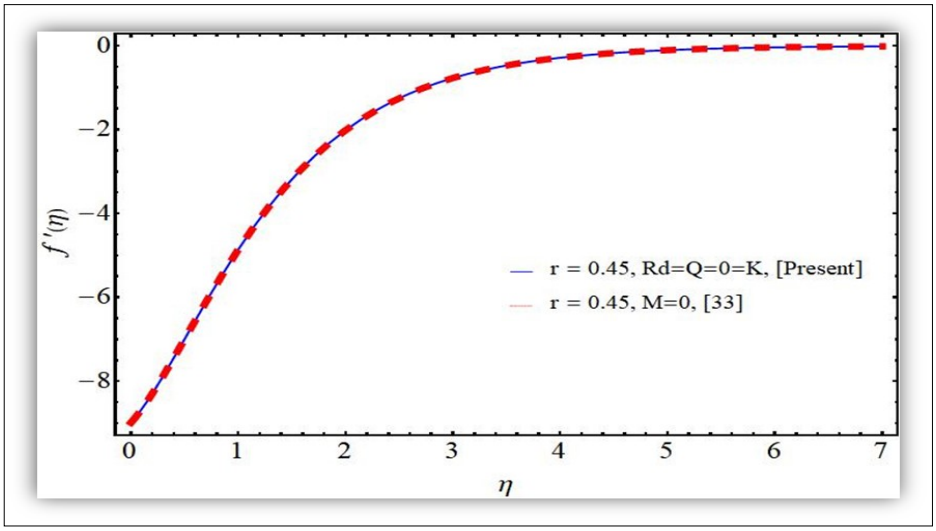

Figure 18. Comparison with [33]

with stronger Marangoni factor (r) however, the elevated values of dimensionless parameter β result in decreasing behavior of flow velocity and the associated boundary layer drops down.

- Prandtl number is an enhancing factor for the temperature distribution.
- Both the radiation and thermophoresis are increasing factors of temperature distribution.
- Chemical reaction forces the away movement of nanoparticles from Riga surface. A prominent decreasing behavior is witnessed with elevated values of *K*.
- Heat flux enhances with augmented values of Thermophoretic factor (Nt).
- Mass flux declines with augmented values of Thermophoretic factor (Nt) and the Prandtl factor (Pr).

References

1. Lin, Y., Zheng, L., Zhang, X., MHD Marangoni boundary layer flow and heat transfer of pseudo-plastic nanofluids over a porous medium with a modified model, Mech Time-Depend Mater, (2015) 4(19) 519-36.
2. Aly, E.H., Ebaid, A., Exact analysis for the effect of heat transfer on MHD and radiation Marangoni boundary layer nanofluid flow past a surface embedded in a porous medium, J Mol Liquids, (2016) 215 625-39.
3. Mat, N.A.A., Arifin, N.M., Nazar, R., Radiation effect on Marangoni convection boundary layer flow of a nanofluid. Mathemat Sci, (2012 1(6) 1-6.
4. Gevorgyan, G.S., Petrosyan, K. A., Hakobyan, R. S., Alaverdyan, R. B., Experimental Investigation of Marangoni Convection in Nanofluids, Journal of Contemporary Physics (Armenian Academy of Sciences), (2017) 4(52) 362â€"365.
5. Abdullah Al-Sharafi, Ahmet, Z. Sahin, Bekir, S. Yilbas, Shuja, S.Z., Marangoni convection flow and heat transfer characteristics of waterâ€"CNT nanofluid droplets, Numerical Heat Transfer, Part A: Applications, (2016) 7(69) 763-780.
6. Choi, S., Enhancing thermal conductivity of fluids with nanoparticles, Developments and Applications of Non-Newtonian Flows. ASME, New York, (1995) 66 99-105.
7. IbÃiÃ±ez, G., LÃ³pez, A., Pantoja, J., Moreira, J., Entropy generation analysis of a nanofluid flow in MHD porous microchannel with hydrodynamic slip and thermal radiation. Int J Heat Mass Trans, (2016) 89-97.
8. Hayat, T., Qayyum, S., Alsaedi, A., Shafiq, A., Inclined magnetic field and heat source/sink aspects in flow of nanofluid with nonlinear thermal radiation. Int J Heat Mass Trans (2016), 103 99-107.
9. Naseem, A., Shafiq, A., Zhao, L., Farooq, M.U., Analytical investigation of third grade nanofluidic flow over a riga plate using Cattaneo-Christov model, Results in Physics, (2018), 9 961-969.
10. Hayat, T., Hussain, S., Muhammad, T., Alsaedi, A., Ayub, M., Radiative flow of Powellâ€"Eyring nanofluid with convective boundary conditions, Chinese Journal of Physics, (2017) 55 1523-1538.
11. Alsabery, A.I., Chamkha, A.J., Saleh, H., Hashim, I., Heatline visualization of conjugate natural convection in a square cavity filled with nanofluid with sinusoidal temperature variations on both horizontal walls, Int. J. Heat Mass Transf, (2016) 100 835-850.
12. Sheikholeslami, M., Ganji, D.D., Heated Permeable Stretching Surface in a Porous Medium Using Nanofluids, Journal of Applied Fluid Mechanics, (2014) 7 535-542.
13. Nasrin, R., Alim, M.A., Chamkha, A.J., Prandtl number and aspect ratio, Int. J. Heat Mass Transf. (2012) 55 7355-7365.
14. Bhatti, M.M., Rashidi, M.M., Effects of thermo-diffusion and thermal radiation on Williamson nanofluid over a porous shrinking/ stretching sheet, J. Mol. Liq. (2016) 221 567-573.
15. Parvin, S., Nasrin, R., Alim, M.A., Hossain, N.F., Chamkha, A.J., Thermal Conductivity Variation on Natural Convection Flow of Water-Alumina Nanofluid in an Annulus, Int. J. Heat and Mass Transf, (2012) 55 5268-5274.
16. Selimefendigil, F., Ã–ztop, H.F., Conjugate natural convection in a cavity with a conductive partition

and filled with different nanofluids on different sides of the partition, J. Mol. Liq, (2016) 216 67-77.

17. RamReddy, C., Murthy, P.V.S.N., Chamkha, A.J., Rashad, A.M., Soret-driven thermosolutal convection induced by inclined thermal and solutal gradients in a shallow horizontal layer of a porous medium, Int. J. Heat and Mass Transf, (2013) 64 384-392.
18. Sheikholeslami, M., Vajravelu, K., Rashidi, M.M., Forced convection heat transfer in a semi annulus under the influence of a variable magnetic field, Int. J. Heat Mass Transf, (2016) 92 339-348.
19. Sheikholeslami, M., Abelman, S., Two phase simulation of nanofluid flow and heat transfer in an annulus in the presence of an axial magnetic field, IEEE Trans. Nanotechnol, (2015) 14 561-569.
20. Sheikholeslami, M., Kandelousi, Influence of Lorentz forces on nanofluid forced convection considering Marangoni convection. Author links open overlay panel, Phys. Lett. A, (2014) 378 3331-3339.
21. Bhatti, M.M., Abbas, T., Rashidi, M.M., El-Sayed, A. M., Numerical simulation of entropy generation with thermal radiation on MHD Carreau nanofluid towards a shrinking sheet, Entropy, (216) 18 200.
22. Bhatti, M.M., Abbas, T., Rashidi, M.M., El-Sayed, A. M., Yang, Z., Generation on MHD Eyring-Powell nanofluid through a permeable stretching surface, Entropy (2016) 18 224.
23. Sheikholeslami, M., Hayat, T., Alsaedi, A., Effects of homogeneous and heterogeneous reactions in flow of nanofluids over a nonlinear stretching surface with variable surface thickness., Int. J. Heat Mass Transf, (2016) 09 077.
24. Sheikholeslami, M., Ganji, D.D., Influence of Lorentz forces on nanofluid forced convection considering Marangoni convection, J. Mol. Liq, (2016) 224 526-537.
25. Sheikholeslami, M., Effect of uniform suction on nanofluid flow and heat transfer over a cylinder, J. Braz. Soc. Mech. Sci. Eng, (2015) 37 1623-1633.
26. Chamkha, A.J., Abbasbandy, S., Rashad, A.M., Vajravelu, K., Radiation effects on mixed convection over a wedge embedded in a porous medium filled with a nanofluid, Transp. Porous Media, (2012) 91 261-279.
27. Sheikholeslami. M, Chamkha. A.J, Flow and convective heat transfer of a ferro-nanofluid in a double-sided lid-driven cavity with a wavy wall in the presence of a variable magnetic field, Numerical Heat Transfer, Part A (2015) 69 1186-1200.
28. Sheikholeslami, M., Chamkha, A.J., Unsteady ferromagnetic liquid flow and heat transfer analysis over a stretching sheet with the effect of dipole and prescribed heat flux., Heat Transfer, Part A, (2016) 69 781-793.
29. Sheikholeslami, M., Ashorynejad, H.R., Rana, P., Simultaneous effects of nanoparticles and slip on Jeffrey fluid through tapered artery with mild stenosis, J. Mol. Liq, (2016) 214 86-95.
30. Sheikholeslami, M., Flow and convective heat transfer of a ferro-nanofluid in a double-sided lid-driven cavity with a wavy wall in the presence of a variable magnetic field, Int. J. Hydrog. Energy, (2016) 09 185.
31. Gailitis, A., Lielausis, O., On a possibility to reduce the hydrodynamic resistance of a plate in an electrolyte, Appl Mag Rep Phys Inst, (1961) 12 143-6.
32. Ahmad, R., Mustafa, M., Turkyilmazoglu, M., Buoyancy effects on nanofluid flow past a convectively heated vertical Riga-plate: A numerical study, Int J Heat and Mass Trans (2017) 111 827-35.
33. Sheikholeslami, M., Chamkha, A.J., Influence of Lorentz forces on nanofluid forced convection considering Marangoni convection, Journal of Molecular Liquids, (2017) 225 750-757.
34. Shafiq, A., Hammouch, Z., Turab, A., Impact of radiation in a stagnation point flow of Waltersâ€™ B fluid towards a Riga plate, Thermal Science and Engineering Progress, (2018) 6 27-33.
35. Adeel, A., Saleem, A., Sumaira, A., Flow of nanofluid past a Riga plate, Journal of Magnetism and Magnetic Materials, (2016) 402 44-48.
36. Ali, I., Rasool, G., Alrashed, S., Numerical simulations of reactionâ€“diffusion equations modeling preyâ€“predator interaction with delay, International Journal of Biomathematics Vol. 11, No. 4 (2018) 1850054.

37. Shijun, L., Homotopy analysis method: A new analytic method for nonlinear problems, Appl Math Mech, (1998) 19 957.
38. Shafiq, A., Nawaz, M., Hayat, T., Alsaedi, A., Magnetohydrodynamic axisymmetric flow of a third-grade fluid between two porous disks, Brazilian Journal of Chemical Engineering (USA), (2013) 3 599-609.
39. Shafiq, A., Jabeen, S., Hayat, T., Alsaedi, A., Cattaneo-Christov heat flux model for squeezed flow of third grade fluid, Surface Review and letters, (2017) 24 1-11.
40. Shafiq, A., Hammouch, Z., Sindhu, T.N., Bioconvective MHD flow of Tangent hyperbolic nano-fluid with Newtonian heating, International Journal of Mechanical Sciences, (2017) 133 759-766.
41. Shafiq, A., Sindhu, T.N., Statistical study of hydromagnetic boundary layer flow of Williamson fluid regarding a radiative surface, Result in Physics, (2017) 7 3059-3067.
42. Malik, R., Khan, M., Shafiq, A., Mushtaq, M., Hussain, M., An analysis of Cattaneo-Christov double-diffusion model for Sisko fluid flow with velocity slip, Journal of Molecular Liquid, (2017) 7 1232-1237